The AB loop and D-helix in binding site III of human Oncostatin M (OSM) are required for OSM receptor activation

Received for publication, January 15, 2018, and in revised form, February 16, 2018 Published, Papers in Press, March 6, 2018, DOI 10.1074/jbc.RA118.001920

Juan M. Adrian-Segarra[1], Natalie Schindler[2], Praveen Gajawada, Holger Lörchner, Thomas Braun[3], and Jochen Pöling[4]

From the Department of Cardiac Development and Remodelling, Max Planck Institute for Heart and Lung Research, 61231 Bad Nauheim, Germany

Edited by Luke O'Neill

Oncostatin M (OSM) and leukemia inhibitory factor (LIF) are closely related members of the interleukin-6 (IL-6) cytokine family. Both cytokines share a common origin and structure, and both interact through a specific region, termed binding site III, to activate a dimeric receptor complex formed by glycoprotein 130 (gp130) and LIF receptor (LIFR) in humans. However, only OSM activates the OSM receptor (OSMR)– gp130 complex. The molecular features that enable OSM to specifically activate the OSMR are currently unknown. To define specific sequence motifs within OSM that are critical for initiating signaling via OSMR, here we generated chimeric OSM–LIF cytokines and performed alanine-scanning experiments. Replacement of the OSM AB loop within OSM's binding site III with that of LIF abrogated OSMR activation, measured as STAT3 phosphorylation at Tyr-705, but did not compromise LIFR activation. Correspondingly, substitution of the AB loop and D-helix in LIF with their OSM counterparts was sufficient for OSMR activation. The alanine-scanning experiments revealed that residues Tyr-34, Gln-38, Gly-39, and Leu-45 (in the AB loop) and Pro-153 (in the D-helix) had specific roles in activating OSMR but not LIFR signaling, whereas Leu-40 and Cys-49 (in the AB loop), and Phe-160 and Lys-163 (in the D-helix) were required for activation of both receptors. Because most of the key amino acid residues identified here are conserved between LIF and OSM, we concluded that comparatively minor differences in a few amino acid residues within binding site III account for the differential biological effects of OSM and LIF.

This work was supported by the Max Planck Society, the Excellence Initiative "Cardiopulmonary System"; Deutsche Forschungsgemeinschaft Collaborative Research Center Pulmonary Hypertension and Core Pulmonale Grants SFB1213, TP A02, and TP B02; Foundation Leducq Grant 3CVD01; the German Center for Cardiovascular Research; and European Research Area Network on Cardiovascular Diseases Grant CLARIFY. The authors declare that they have no conflicts of interest with the contents of this article.

This article contains Figs. S1–S3 and Table S1.

[1] Supported by CardioNeT (Marie Curie ITN-2011-GA: 289600) and the Loewe-Zentrum Universities of Gießen and Marburg Lung Center (UGMLC).

[2] Present address: Institut für Entwicklungsbiologie und Neurobiologie (IDN), Fachbereich Biologie (FB 10), Johannes Gutenberg University Mainz, Germany c/o Institute of Molecular Biology gGmbH (IMB), 55128 Mainz, Germany.

[3] To whom correspondence may be addressed: Dept. of Cardiac Development and Remodeling, Max Planck Institute for Heart and Lung Research, Ludwigstr. 43, 61231 Bad Nauheim, Germany. Tel.: 49-6032-705-1102; Fax: 49-6032-705-1104; E-mail: thomas.braun@mpi-bn.mpg.de.

[4] To whom correspondence may be addressed: Dept. of Cardiac Development and Remodeling, Max Planck Institute for Heart and Lung Research, Ludwigstr. 43, 61231 Bad Nauheim, Germany. Tel.: 49-6032-705-1106; Fax: 49-6032-705-1104; E-mail: jochen.poeling@mpi-bn.mpg.de.

The IL-6[5] class of cytokines is formed by ten different members: IL-6, IL-11, IL-27, IL-31, ciliary neurotrophic factor, cardiotrophin-1, cardiotrophin-like cytokine, neuropoietin, LIF, and OSM (1–9). They all display a common secondary structure comprised of four helices joined by loops to form a bundle (10–13). These cytokines exert their actions by binding to oligomeric receptor complexes formed by gp130 and one or more specific co-receptors, including LIFR and OSMR (14). Activated receptor complexes initiate distinct signaling events by recruiting and phosphorylating components of the mitogen-activated protein kinases (MAPKs), the phosphoinositide 3-kinase/protein kinase B (PI3K/Akt) and the Janus kinase/signal transducer and activator of transcription (JAK/STAT) pathways (15).

LIF and OSM are the most closely related members of the IL-6 family and originated from the same ancestral gene after a duplication event (Fig. 1, *A* and *B*) (16–18). OSM and LIF both induce formation of a heteromeric LIFR– gp130 receptor complex (3, 19), albeit by different mechanisms. LIF interacts first with the LIFR before gp130 is recruited and the heteromeric complex forms. In contrast, OSM binds first to gp130 before recruiting the LIFR (3, 20, 21). After binding to gp130, OSM might alternatively recruit the OSMR to induce OSMR– gp130 complex formation, which is not accomplished by any other cytokine (20).

Intriguingly, the interaction of OSM with either OSMR or LIFR is mediated through the same region, termed binding site III, which comprises the N-terminal region of helix D and the loops between helices A-B and B-C (Fig. 1*C*) (13). The specific details regarding these interactions, however, remain elusive because no structural data of OSM binding to any of its receptors have been obtained (22). Based on site-directed mutagenesis experiments, it has been claimed that a conserved F*XX*K motif in helix D of OSM is essential for both LIFR and OSMR binding (13), although this motif alone is also present in LIF and all other LIFR-binding cytokines and therefore does not explain the specific interaction of OSM with OSMR (Fig. 1*D*) (23). One of the main differences between OSM and LIF is the size of the BC loop, but shortening OSM's longer BC loop does not influence the ability of OSM to bind to the OSMR (21).

[5] The abbreviations used are: IL-6, interleukin-6; LIF, leukemia inhibitory factor; OSM, Oncostatin M; LIFR, leukemia inhibitory factor receptor; OSMR, Oncostatin M receptor; STAT, signal transducer and activator of transcription; cDNA, complementary DNA; DMEM, Dulbecco's modified Eagle's medium.

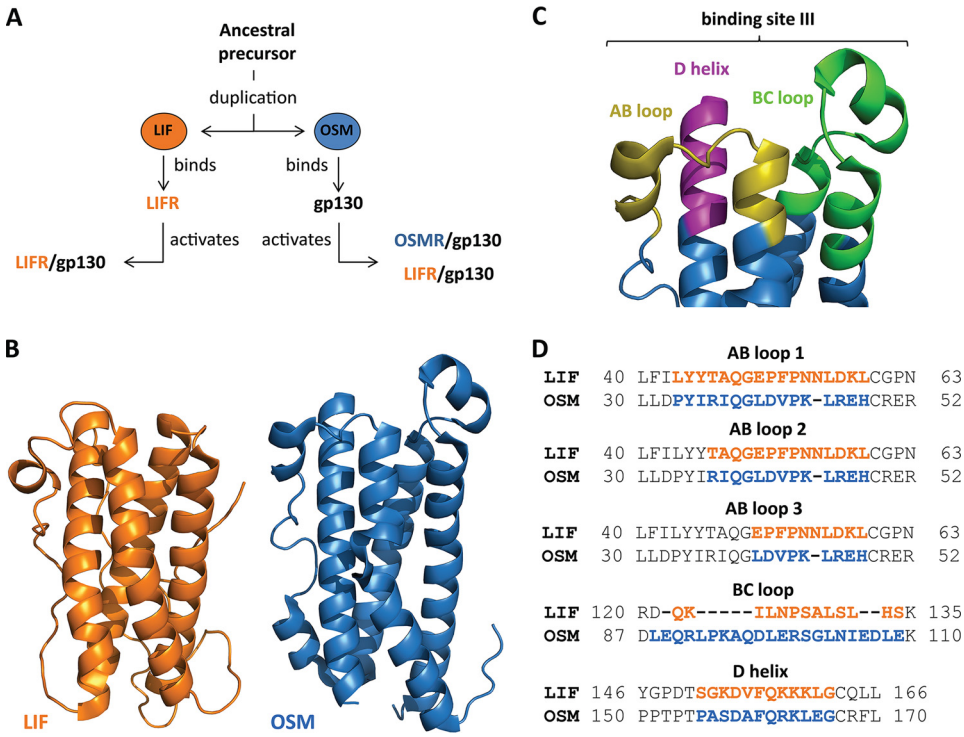

Figure 1. Comparison of the structures of OSM and LIF. *A*, OSM and LIF share a common evolutionary origin but activate different receptors. *B*, representation of the crystal structures of OSM (PDB code 1EVS) and LIF (PDB code 2Q7N). *C*, binding site III of OSM is formed by parts of the AB loop, the BC loop, and the D-helix. *D*, alignment of the different regions in binding site III of OSM and LIF, which were exchanged to construct different OSM–LIF chimeras.

Here we examined the molecular characteristics of the OSM binding site III that are critical for activation of specific receptors. The importance of different regions of OSM binding site III for OSMR activation was examined by creating chimeric cytokines (24). Exchange of the AB loop and N-terminal D-helix regions in LIF with corresponding regions from OSM generated a chimeric LIF cytokine that initiated OSMR signaling. Because our results suggested a critical role of the AB and D loops, we conducted a detailed alanine site-directed mutagenesis scan, which led to the identification of Tyr-34, Gln-38, Gly-39, and Leu-45 in the AB loop and Pro-153 in the D-helix of OSM as key residues for specific OSMR activation. Alignment of the binding sites III of OSM and LIF revealed that most of the critical residues are conserved between both molecules. We therefore argue that differences in the spatial organization of a few amino acid residues within binding site III of OSM and LIF cause divergent receptor activation.

Results

Design and production of OSM–LIF chimeric cytokines

The OSM and LIF residues forming different helices and loops are well known because of the available crystal structures of human OSM (PDB 1EVS) and LIF (PDB 2Q7N) (13, 21, 25). In contrast, the functional boundaries of OSM binding site III have not been defined precisely. To design replacements within the AB loop, BC loop, and D-helix regions of binding site III, we aligned the amino acid sequences of human OSM and human LIF using ClustalW (26). The conserved Cys residues required for disulfide bond formation were selected as the C-terminal amino acids of the AB loop and D-helix, and the conserved Thr residue N-terminal of the F*XX*K motif was chosen as a starting point for the D-helix replacement. Because no characteristic amino acid demarcating the start of the AB loop was evident, three different replacement lengths were selected. We chose a rather large region comprising the C terminus of helix B and the N terminus of helix C, starting with an Asp and ending with a conserved Lys residue, because shortening of the central region of the BC loop does not impair OSMR activation (21) (Fig. 1*D*).

In *Escherichia coli* expression systems, OSM forms insoluble inclusion bodies, requiring extra steps for purification (27). We hypothesized that aggregation and misfolding in prokaryotes might be facilitated by the reducing redox state preventing formation of critical disulfide bond between helices A and D of OSM (28). Hence, we used a modified *E. coli* strain expressing a chaperone/disulfide bond isomerase (29), which produced high yields of soluble, biologically active OSM as well as the various OSM point mutants. In contrast, we were unable to recover sufficient quantities of OSM–LIF chimeras from either *E. coli* strain (data not shown) and therefore switched, for the expression of chimeric molecules, to a mammalian system based on FreeStyle 293-F cells.

Assessment of receptor activation by OSM or LIF

OSM does not interact with OSMR in the absence of gp130, which renders determination of OSM-OSMR binding affinity difficult (20, 30). However, measurement of the phosphorylation level of downstream signaling molecules, such as STAT3, offers an alternative (31). We employed human cell lines specifically expressing only either OSMR (A375 melanoma cells) or LIFR (JAR choriocarcinoma cells) (32) and determined STAT3 Tyr-705 phosphorylation 10 min after stimulation. To

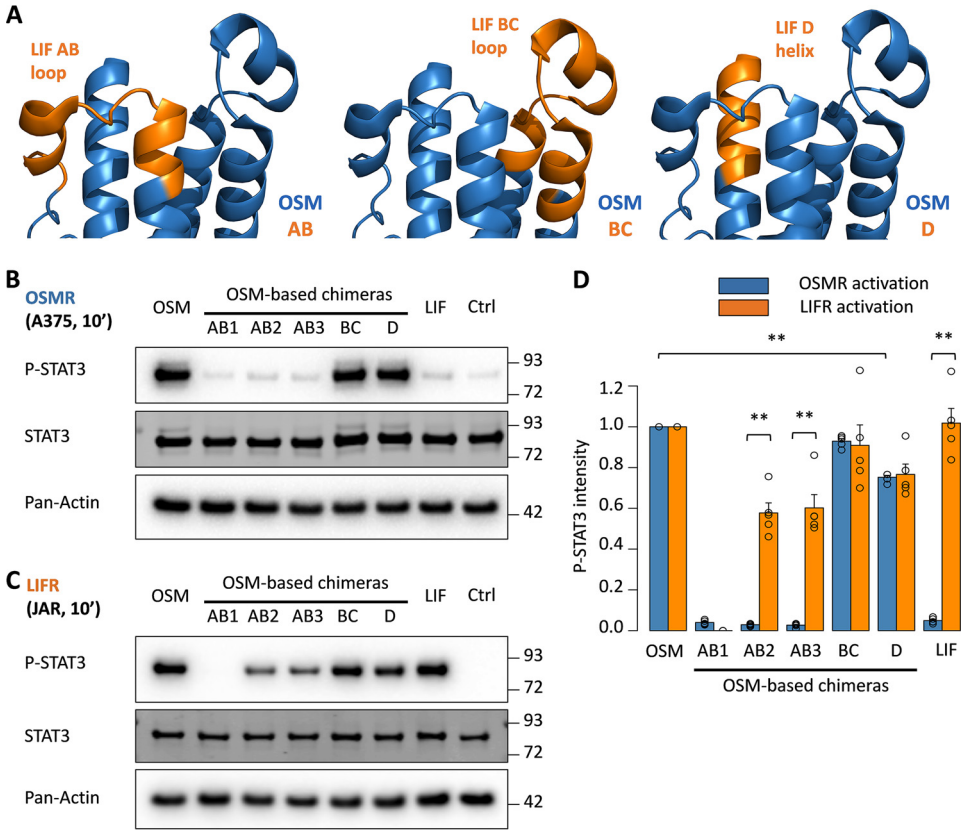

Figure 2. The AB loop of OSM is required for short-term OSMR activation. *A*, depiction of the different domain swaps in OSM-based chimeras using corresponding LIF counterparts. *B* and *C*, STAT3 phosphorylation levels in A375 cells (OSMR activity) and JAR cells (LIFR activity) 10 min after cytokine stimulation. *Ctrl*, control. *D*, relative quantification of receptor activation by each chimeric cytokine. P-STAT3 band intensities were first normalized against total STAT3 levels. Data were then transformed relative to the basal (control) signal, which was set to 0. Values are presented as mean ± S.E., $n = 5$ independent cultures; **, $p < 0.01$.

ascertain that only the OSMR or LIFR induced STAT3 phosphorylation, either of the receptors was inactivated by specific siRNAs (Fig. S1). In addition to STAT3 phosphorylation we also measured the expression of tissue inhibitor of metalloproteinase 1 (TIMP1) and total STAT3 levels after 24 h, which increase as a result of prolonged OSMR and LIFR stimulation, respectively (33, 34). Similar to the short-term stimulation studies, siRNA inhibition experiments were used to demonstrate the specificity of these markers (Fig. S2). Finally, we quantified the well-known effects of OSMR activation on the proliferation of A375 cells as a biological readout (35).

The AB loop of OSM is required for OSMR activation

To identify critical regions for receptor activation, we first generated OSM-based chimeric cytokines in which different sections of OSM were replaced by corresponding parts of the LIF molecule (Fig. 2*A*). The OSM–LIF chimeras were first tested in a short-term cell stimulation assay. Interestingly, the AB2 and AB3 OSM–LIF chimeras activated the LIFR in JAR cells but not the OSMR in A375 cells (Fig. 2, *B* and *C*), clearly indicating that the AB loop is crucial for the specificity of OSM-OSMR interaction. The AB1 OSM–LIF chimera, which contains a longer AB loop replacement, failed to activate either the LIFR or OSMR, probably because of disruption of the secondary structure (Fig. 2, *B* and *C*). In contrast to the AB loop chimeras, and in line with previous reports, exchange of the BC loop had no measurable impact on the activation of either receptor, whereas exchange of the N-terminal D-helix caused a small but statistically significant reduction in the signaling activity of both OSMR and LIFR (Fig. 2, *B–D*).

Nearly identical results were obtained in long-term stimulation experiments in which OSMR-mediated TIMP1 expression in HepG2 cells was induced by native OSM, the BC loop chimera, and, to a lesser degree, by the D-helix chimera but not by the AB loop chimeric cytokines (Fig. 3*A*). Similar to the short-term stimulation experiments, AB2 and AB3 variants activated LIFR signaling to the same extent as native LIF in JAR cells, as indicated by increased STAT3 levels, but failed to increase OSMR-dependent TIMP1 levels in HepG2 cells (Fig. 3, *B* and *C*). Likewise, native OSM and the BC loop and D-helix chimeras, but not the AB loop variants, inhibited proliferation of A375 cells through OSMR activation (Fig. 3*D*).

Exchange of binding site III in LIF by corresponding OSM sequences enables OSMR activation

So far, our experiments indicated that the AB loop region in binding site III of OSM is required for OSMR activation but did not rule out the existence of other essential regions outside of binding site III. Therefore, we exchanged different regions of binding site III in LIF and not in OSM as before (Fig. 4*A*). Interestingly, replacement of the N-terminal AB loop region alone was not sufficient for LIF to acquire the ability to initiate OSMR

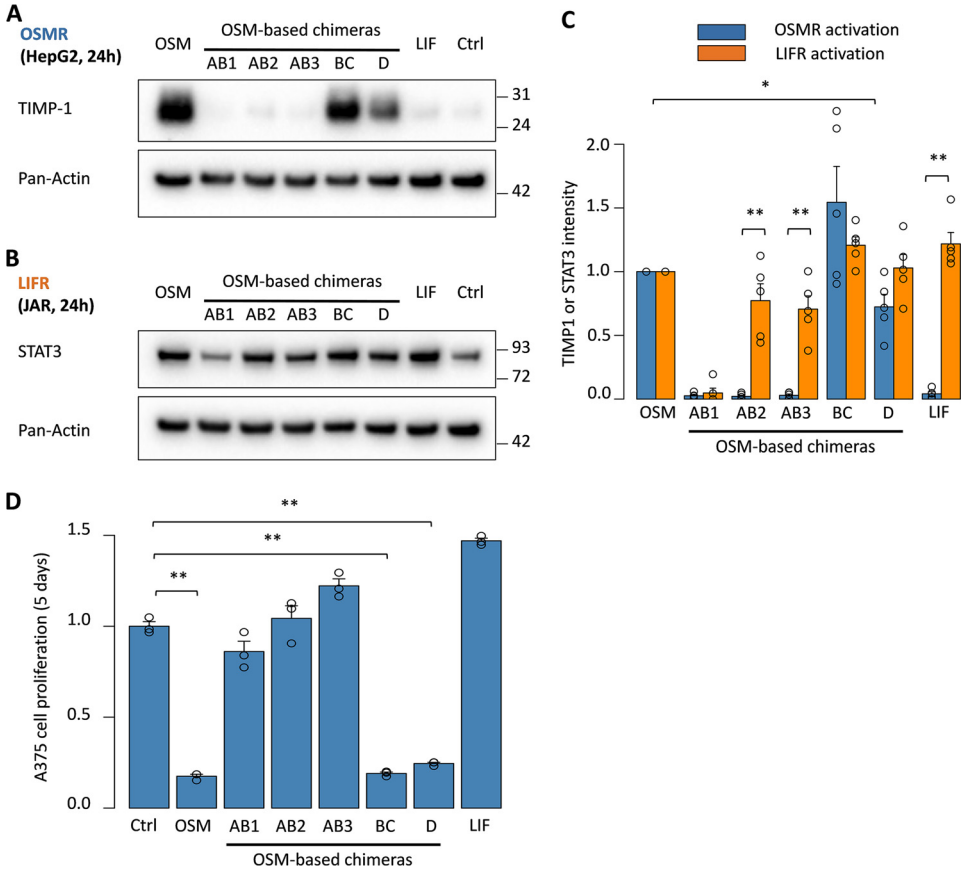

Figure 3. The AB loop of OSM is required for long-term OSMR activation. *A* and *B*, TIMP1 levels in HepG2 cells (OSMR activity) and STAT3 levels in JAR cells (LIFR activity) 24 h after chimeric cytokine stimulation. *Ctrl*, control. *C*, relative quantification of receptor activation by each chimeric cytokine. TIMP1 and STAT3 band intensities were first normalized against pan-Actin levels. Data were then transformed relative to the basal (control) signal, which was set to 0. Values are presented as mean ± S.E., $n = 5$ independent cultures; **, $p < 0.01$. *D*, A375 cell proliferation after 5-day cytokine stimulation, normalized to the proliferation of untreated cells. Values are presented as mean ± S.E., $n = 3$ independent cultures; **, $p < 0.01$.

signaling (Fig. 4*B*). Only the chimera with both AB loop and D-helix substitutions led to STAT3 phosphorylation in A375 cells 10 min after stimulation, albeit at lower levels than native OSM (Fig. 4*B*). In contrast, every chimera generated was active through the LIFR receptor, again suggesting the absence of major conformational changes in these mutant cytokines (Fig. 4, *C* and *D*).

These observations were subsequently reinforced by long-term stimulation experiments. Only the AB+D chimeric LIF proved capable of up-regulating TIMP1 expression in HepG2 cells after 24 h (Fig. 5, *A–C*) or of inhibiting A375 cell proliferation after 5 days (Fig. 5*D*), thus confirming these two regions of binding site III of OSM as the main differentiating feature between OSM and other IL-6 family members in receptor activation.

Identification of amino acid residues within the AB loop of OSM playing key roles in OSMR activation

To characterize the contribution of individual amino acid residues within the AB loop of OSM for OSMR activation, we pursued an alanine-scanning approach (36). Individual point mutants were generated in the N-terminal AB loop of OSM from Pro-33 to Cys-49 by replacing each amino acid with an alanine and tested in short-term stimulation experiments. Only two substitutions, L40A and the already described C49A (28), disrupted the ability of OSM to activate OSMR or LIFR (Fig. 6, *A–C*). In contrast, alanine replacement of Tyr-34, Gln-38, Gly-39, and Leu-45 in OSM prevented only OSMR but not LIFR signaling, as indicated by the differential effects on STAT3 phosphorylation in OSMR- and LIFR-expressing A375 and JAR cells, respectively (Fig. 6, *A–C*).

Long-term stimulation experiments yielded similar results: the Q38A, G39A, L45A, and, to a lesser extent, the Y34A mutant showed an absence of OSMR-dependent induction of TIMP1 expression in HepG2 cells but normal STAT3 up-regulation in JAR cells, whereas the L40A and C49A mutants were unable to activate either receptor (Fig. 7, *A–C*). Unlike WT OSM, the Y34A, Q38A, G39A, and L45A mutants did not inhibit proliferation of A375 cells, further confirming the importance of these residues for OSMR signaling initiation (Fig. 7*D*).

Role of individual amino acid residues in the D-helix of OSM for OSMR activation

The requirement of the N-terminal D-helix region in LIF-based chimeras for efficient OSMR signaling suggested the existence of critical amino acids outside the conserved F*XX*K motif for OSMR activation. To identify corresponding residues, each amino acid in the replaced D-helix was substituted by an alanine. The P153A mutant showed a 4-fold reduction of

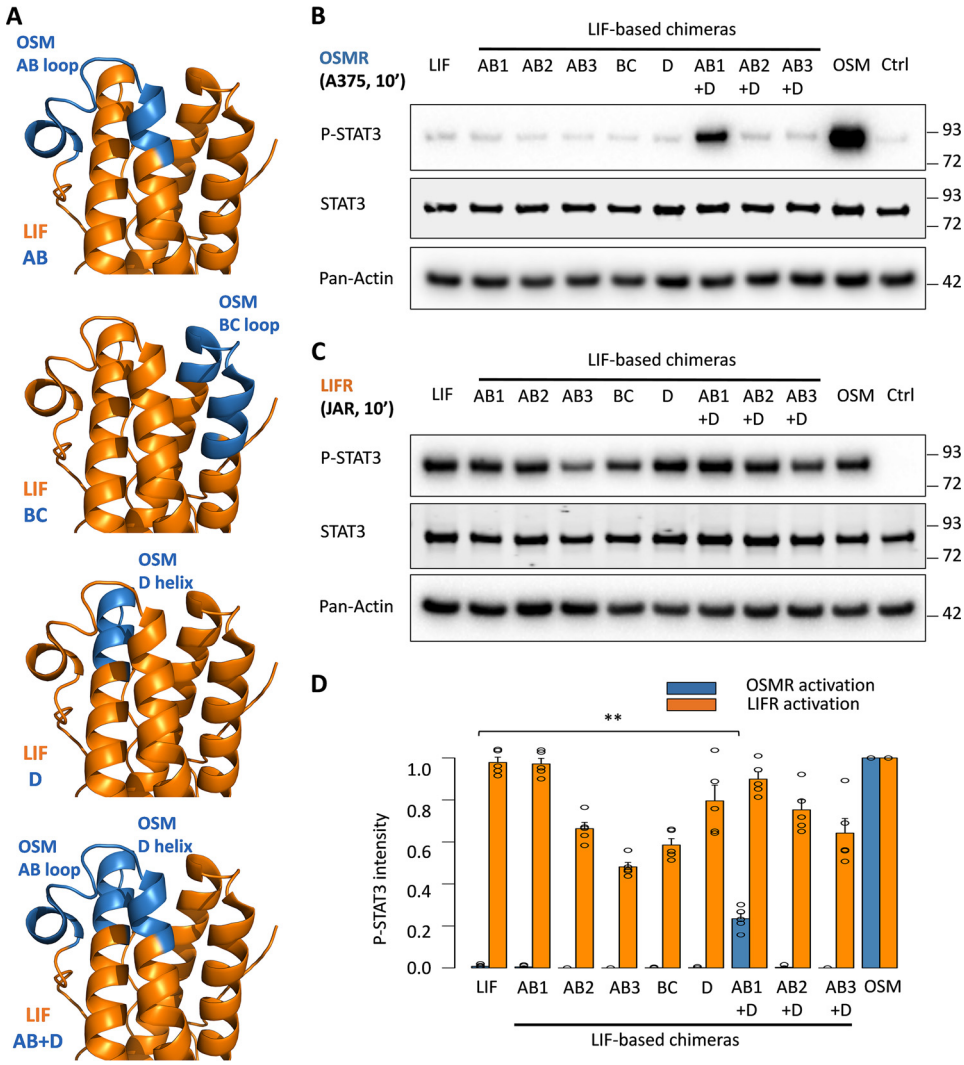

Figure 4. Exchange of binding site III in LIF by OSM sequences enables short-term OSMR activation. *A*, depiction of the different domain swaps in LIF-based chimeras using corresponding OSM counterparts. *B* and *C*, STAT3 phosphorylation levels in A375 cells (OSMR activity) and JAR cells (LIFR activity) 10 min after stimulation. *Ctrl*, control. *D*, relative quantification of receptor activation by each chimeric cytokine. P-STAT3 band intensities were first normalized against total STAT3 levels. Data were then transformed relative to the basal (control) signal, which was set to 0. Values are presented as mean ± S.E., $n = 5$ independent cultures; **, $p < 0.01$.

STAT3 phosphorylation in short-term stimulation assays in A375 cells relative to WT OSM but normal P-STAT3 levels in JAR cells (Fig. 8, *A–C*). In addition to P153A, only the F160A and K163A mutations, which change the F*XXK* motif, had a significant effect. However, unlike P153A, F160A and K163A prevented activation of both OSMR and LIFR (Fig. 8, *A–C*). Long-term stimulation experiments confirmed these results, showing reduced OSMR-dependent TIMP1 expression in HepG2 cells but normal LIFR-dependent up-regulation of STAT3 by P153A (Fig. 9 *A–C*). Likewise, P153A did not inhibit proliferation of the A375 cell line compared with WT OSM (Fig. 9*D*).

The amino acid residues necessary for OSMR activation are conserved between human OSM and LIF and form a spatial cluster

The identification of individual amino acids in the N-terminal AB loop and D-helix regions critical for OSMR but not LIFR activation suggested that such amino acids might not be conserved between OSMR and LIFR. Surprisingly, however, sequence alignment of the two cytokines revealed that Tyr-34, Gln-38, Gly-39, and Leu-45, in addition to the F*XXK* motif, were conserved between OSM and LIF. To answer this riddle, we examined the position of Tyr-34, Gln-38, Gly-39, and Leu-45 in the crystal structures of OSM and LIF (Fig. 10). We found that, in LIF, the corresponding Gly-39 and Leu-45 residues are separated by an extra amino acid, which is missing in the OSM AB loop. The resulting conformational changes seem to disrupt the main OSMR interaction site, which contains the critical Tyr-34, Gln-38, Gly-39, and Leu-45 amino acid residues, as evidenced by the surface rendering of the molecules (Fig. 10). In addition, the surface charge of binding site III, likely influenced by these conformational changes, differs in OSM and LIF (13 and Fig. S3). We concluded that the different spatial organization of Tyr-34, Gln-38, Gly-39, and Leu-45, because of the insertion of an additional amino acid into binding site III, plays an important role in the differential biological effects of OSM and LIF.

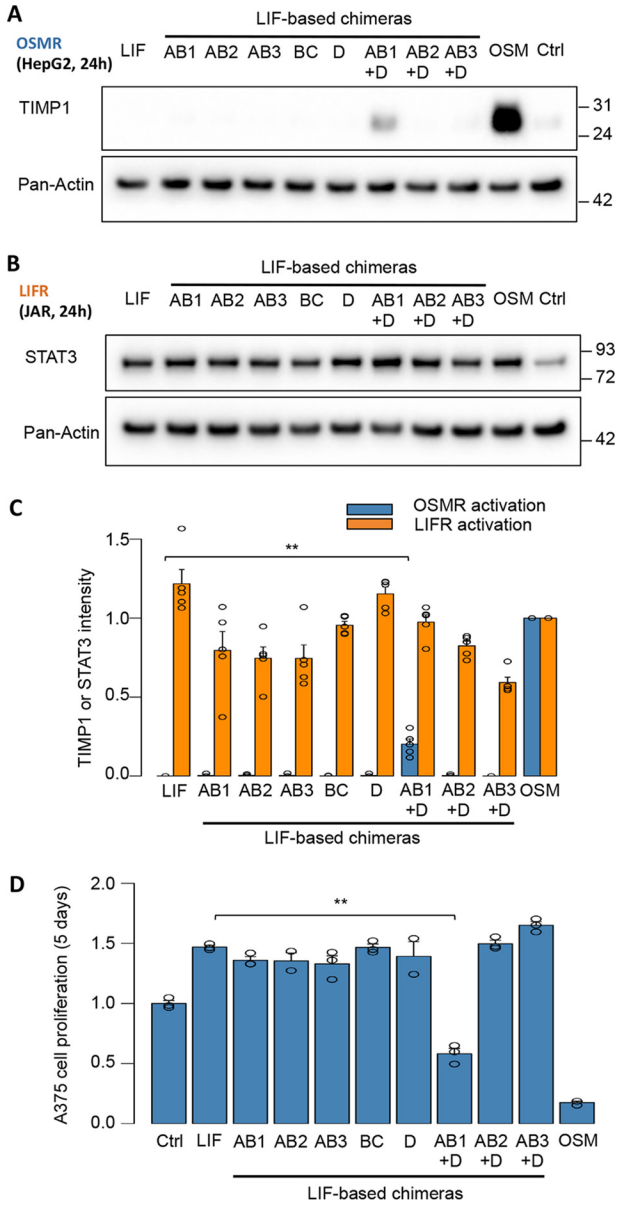

Figure 5. Exchange of binding site III in LIF by OSM sequences enables long-term OSMR activation. *A* and *B*, TIMP1 levels in HepG2 cells (OSMR activity) and STAT3 levels in JAR cells (LIFR activity) 24 h after chimeric cytokine stimulation. *Ctrl*, control. *C*, relative quantification of receptor activation by each chimeric cytokine. TIMP1 and STAT3 band intensities were first normalized against pan-Actin levels. Data were then transformed relative to the basal (control) signal, which was set to 0. Values are presented as mean ± S.E., $n = 5$ independent cultures; $^{**}p < 0.01$. *D*, A375 cell proliferation after 5-day cytokine stimulation, normalized to the proliferation of untreated cells. Values are presented as mean ± S.E., $n = 3$ independent cultures; **, $p < 0.01$.

Discussion

Activation of OSMR–gp130 signaling distinguishes OSM from all other IL-6 family members (20, 22). However, only few details about the OSM-OSMR interactions were known so far. It was described that the BC loop and N-terminal parts of the AB loop and D-helix of OSM, termed binding site III, form contacts with both the OSMR and the LIFR (13). Furthermore, it was reported that the conserved F*XX*K motif in the D-helix of OSM mediates activation of both receptor complexes, but the features distinguishing OSM from LIF and other LIFR-activating cytokines remained enigmatic (13, 21). In this work, we generated several OSM–LIF and LIF–OSM chimeras to demonstrate that OSMR activation depends on the N-terminal AB loop and D-helix of OSM. The specific loss of OSMR signaling activity in some chimeras revealed a more stringent ligand–receptor interaction for OSM and OSMR compared with LIFR and its ligands. The more adaptive structure of LIFR seems to allow activation by different cytokines, whereas activation of OSMR–gp130 is confined to OSM (37).

Our results using LIF–OSM chimeras, in which the whole binding site III of OSM was inserted into LIF, indicated that binding site III is not only required but also sufficient for OSMR activation. These findings seem to suggest the existence of evolutionarily selected receptor binding modules that determine specific ligand–receptor interactions. Such a model has been proposed for ciliary neurotrophic factor, another IL-6 family member, which contains a LIFR-binding site (24). However, we noticed that the ability of LIF-based OSM chimeras to activate OSMR was lower compared with WT OSM, which suggests a role for additional domains in OSM outside of binding site III. Such additional domains might also account for the markedly higher affinity of OSM compared with LIF for gp130 (3). It seems likely that the impact of domains outside of binding site III is also responsible for the different effects of D-helix exchanges in OSM-based and LIF-based chimeras. In this context, we would like to speculate that domains outside of binding site III partially compensate for replacement of the D-helix in OSM chimeras, which results in only minor changes in OSMR activation. The absence of such compensatory features in LIF-based chimeras might magnify even slight deviations in the AB loop and D-helix orientations and, thereby, strongly compromise receptor activation.

Detailed analysis of the contribution of individual residues within the AB loop region for OSMR activation identified the amino acids Gln-38, Gly-39, and Leu-45 as particularly relevant, whereas the Y34A point mutant reduced, but did not abolish, OSMR activation. Other mutations, such as L40A and C49A, eliminated activation of both OSMR and LIFR. Some of these amino acids (leucine, glycine) are nonpolar and thus unlikely to participate in direct OSM–OSMR interactions. More frequently, these residues play a role in maintaining a protein's secondary structure (38–40). We assume that Gln-38, Gly-39, Leu-40, and Leu-45 are required to establish the proper spatial organization of the AB loop necessary for receptor activation. This notion is further reinforced by the identification of P153 in the N-terminal D-helix as exclusively impacting OSMR activation. Proline and glycine are often found in tight turns in secondary structures (38). Hence, replacing either Gly-39 or Pro-153 with alanine will alter the spatial arrangement of binding site III, probably not to a major extent because the LIFR is still activated, but sufficiently to flunk the rigid needs of OSMR activation.

To our surprise, the majority of OSM residues required for OSMR activation are conserved in LIF. However, closer inspection of the crystal structures indicated that the conserved amino acids show different spatial arrangements in OSM and LIF molecules, largely caused by absence of a residue between Gly-39 and Leu-45 in OSM compared with LIF. This resulted in a lack of surface accessibility of the equivalent Leu-56 in LIF, which constitutes a critical difference within binding site III of

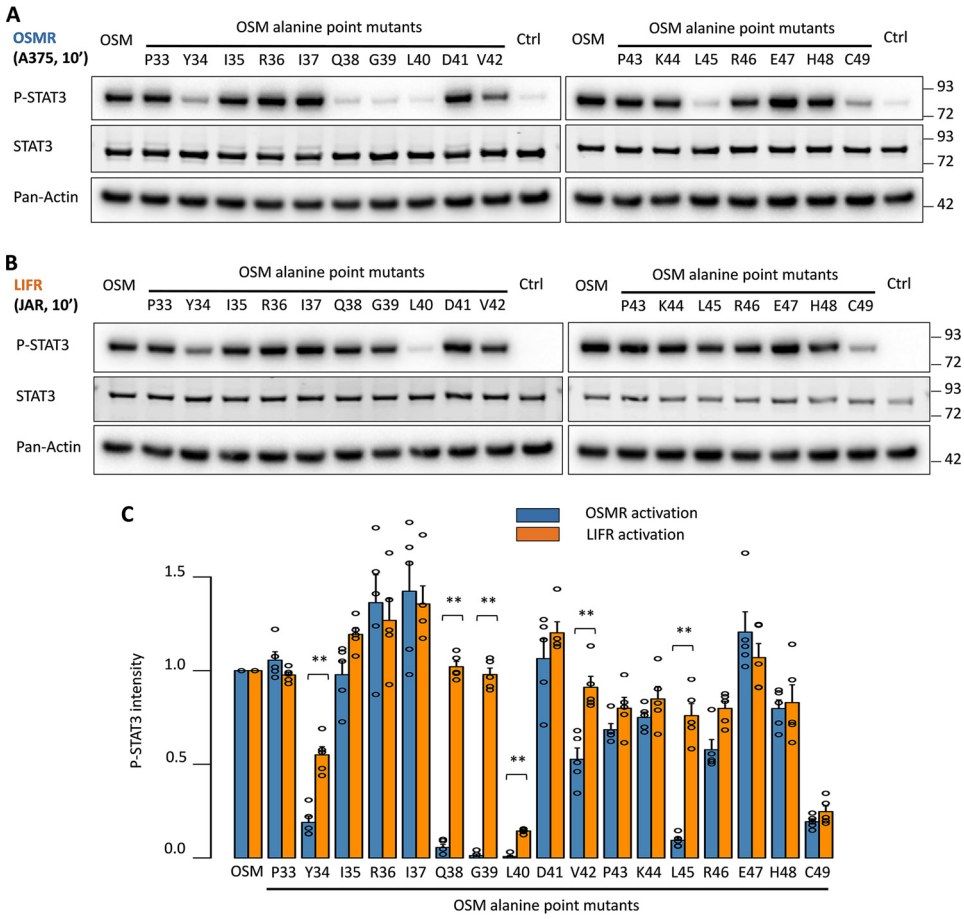

Figure 6. Specific residues in the AB loop of OSM determine short-term receptor activation. *A* and *B*, STAT3 phosphorylation levels in A375 cells (OSMR activity) and JAR cells (LIFR activity) 10 min after stimulation with OSM AB loop alanine point mutants. *Ctrl*, control. *C*, relative quantification of receptor activation by each point mutant. P-STAT3 band intensities were first normalized against total STAT3 levels. Data were then transformed relative to the basal (control) signal, which was set to 0. Values are presented as mean ± S.E., $n = 5$ independent cultures; **, $p < 0.01$.

these cytokines. It appears likely that a relatively small number of mutations in the common ancestor gene for OSM and LIF led to structural changes in the original binding site III, allowing different ligand–receptor interactions.

Our structure–function study of OSM with its receptors OSMR and LIFR is based on several different functional readouts (STAT3 phosphorylation, STAT3 and TIMP1 protein levels, and inhibition of cell proliferation). It should be noted that all of these effects are dependent on STAT3 activation. Preliminary experiments by our group (data not shown) indicate the ability of the LIF–OSM chimera to initiate other signaling pathways downstream of OSMR such as STAT1, but it remains possible that some of the results reported here apply exclusively to STAT3 specificity. We also tried to determine binding affinities of different OSM mutants to OSMR and LIFR, but we were unable to obtain convincing results. Hence, it is still possible that loss of receptor activation is not solely due to an absence of cytokine receptor binding. In principle, the OSM mutants might still retain receptor binding ability but might be unable to induce the required conformational changes for induction of downstream signaling. Crystal structures, other high-resolution structural information about the cytokine-binding site of OSMR, or co-crystallization of OSM with its receptors might help in this regard (22). Another intriguing aspect of OSM biology is the reported species specificity. Human and rat OSM signal both via OSMR and LIFR complexes, apparently activating similar downstream signaling pathways (20, 41). Mouse OSM was long thought to be OSMR-specific, but recent data suggest that mouse OSM also activates LIFR, albeit by different intracellular signaling mechanisms (42, 43). So far, no clear explanation is available for the divergent OSM–LIFR interactions between mouse and human.

OSMR–gp130 signaling has been implicated in numerous physiological and pathological processes (reviewed in Ref. 22). OSM plays important roles in liver homeostasis and metabolism, inflammation, hematopoiesis, and bone remodeling, among others (30, 44–48). Especially interesting is the involvement of OSMR-dependent signaling in different disease conditions (49). Short-term OSMR activation has protective effects in different ischemic injury models (50–54), which makes OSM an attractive pharmacological target. In the course of this study, we have established robust protocols for the production and recovery of recombinant OSM that provide several advantages compared with previous reports, including the production of mutant OSM versions with an altered target spectrum (13, 27). In contrast to short-term OSM signaling, continuous OSMR–gp130 activation has been associated with pathologies such as inflammatory bowel disease, glioblastoma, and dilated car-

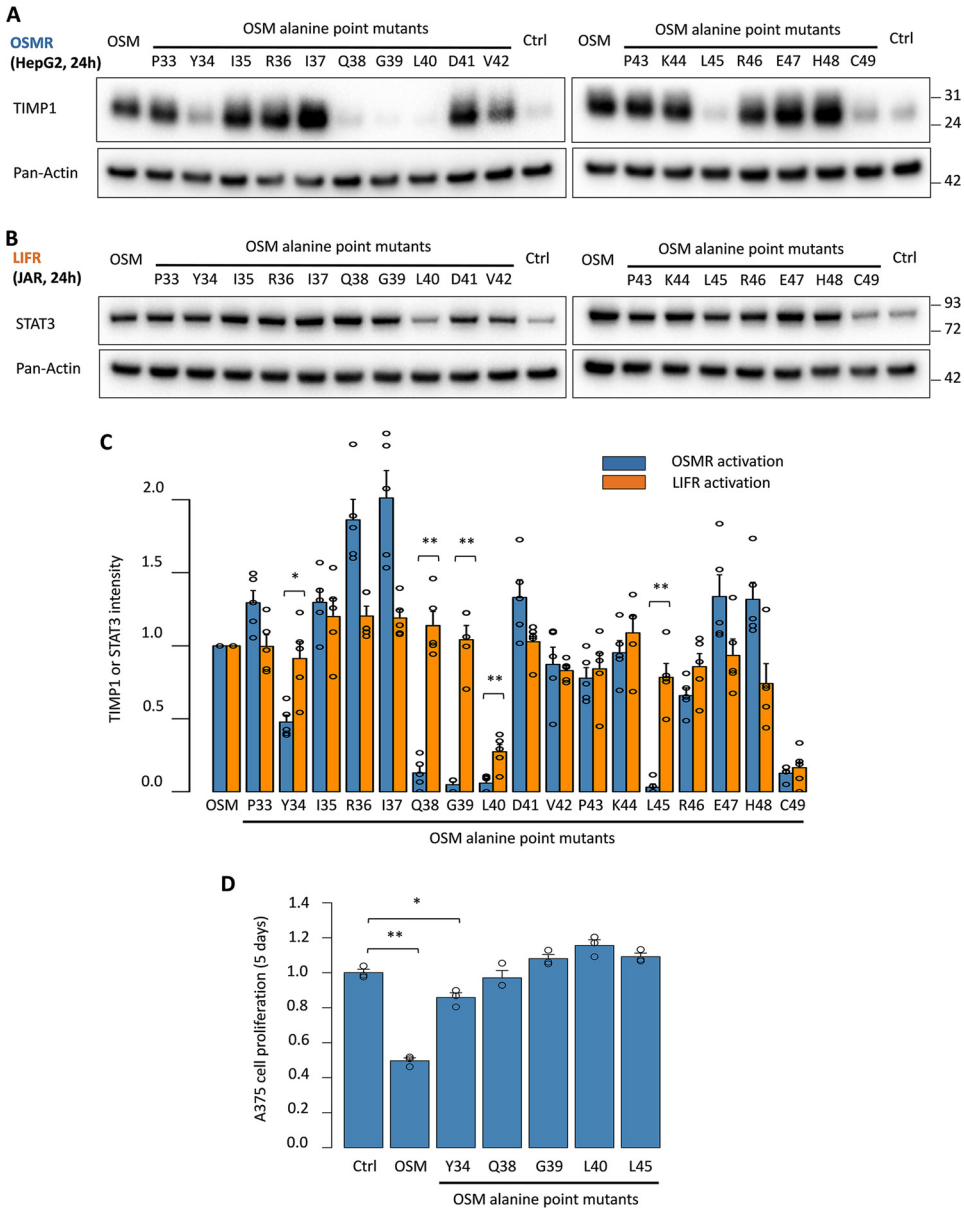

Figure 7. Point mutations in selected OSM AB loop amino acids modulate long-term receptor activation. *A* and *B*, TIMP1 levels in HepG2 cells (OSMR activity) and STAT3 levels in JAR cells (LIFR activity) 24 h after OSM AB loop alanine point mutant stimulation. *Ctrl*, control. *C*, relative quantification of receptor activation by each point mutant: TIMP1 and STAT3 band intensities were first normalized against pan-Actin levels. Data were then transformed relative to the basal (control) signal, which was set to 0. Values are presented as mean ± S.E., $n = 5$ independent cultures; **, $p < 0.01$. *D*, A375 cell proliferation after 5-day cytokine stimulation with selected alanine point mutants, normalized to the proliferation of untreated cells. Values are presented as mean ± S.E., $n = 3$ independent cultures; *, $p < 0.05$; **, $p < 0.01$.

diomyopathy. For such conditions, specific inhibition of OSMR activity might improve the clinical course (55–57). Neutralizing OSMR-specific antibodies might be an option to achieve this goal but are not without drawbacks (56, 57) because OSMR also forms complexes with co-receptors other than gp130, such as IL-31 receptor α (58). Hence, antibodies against OSMR will not only prevent OSMR–gp130 activation but also additional signaling pathways. The insights obtained by our detailed analysis of OSM–OSMR interactions provide valuable information for the design of specific inhibitors of OSM signaling. Particularly attractive in this regard is the finely tuned modification of the 3D structure of binding site III. We believe that our findings provide a significant step forward to bring specific OSMR–gp130 activation and inhibition strategies to clinical application.

Experimental procedures

Chimera construction and site-directed mutagenesis

Human OSM cDNA was a kind gift from Dr. Heike Hermanns (University of Würzburg), whereas human LIF cDNA (MHS6278-202857165) was purchased from Thermo Fisher Scientific. For prokaryotic expression, OSM and LIF were amplified by PCR, flanked by NdeI and XhoI restriction sites, and cloned into the pET-26b(+) vector containing a His_6 tag. Chimeras were constructed by overlapping PCR, first generating the different fragments forming each chimera with overlapping regions of 30 nucleotides, which were then used as a template for a second PCR reaction to obtain the desired gene sequence flanked by NdeI and XhoI restriction sites. Site-di-

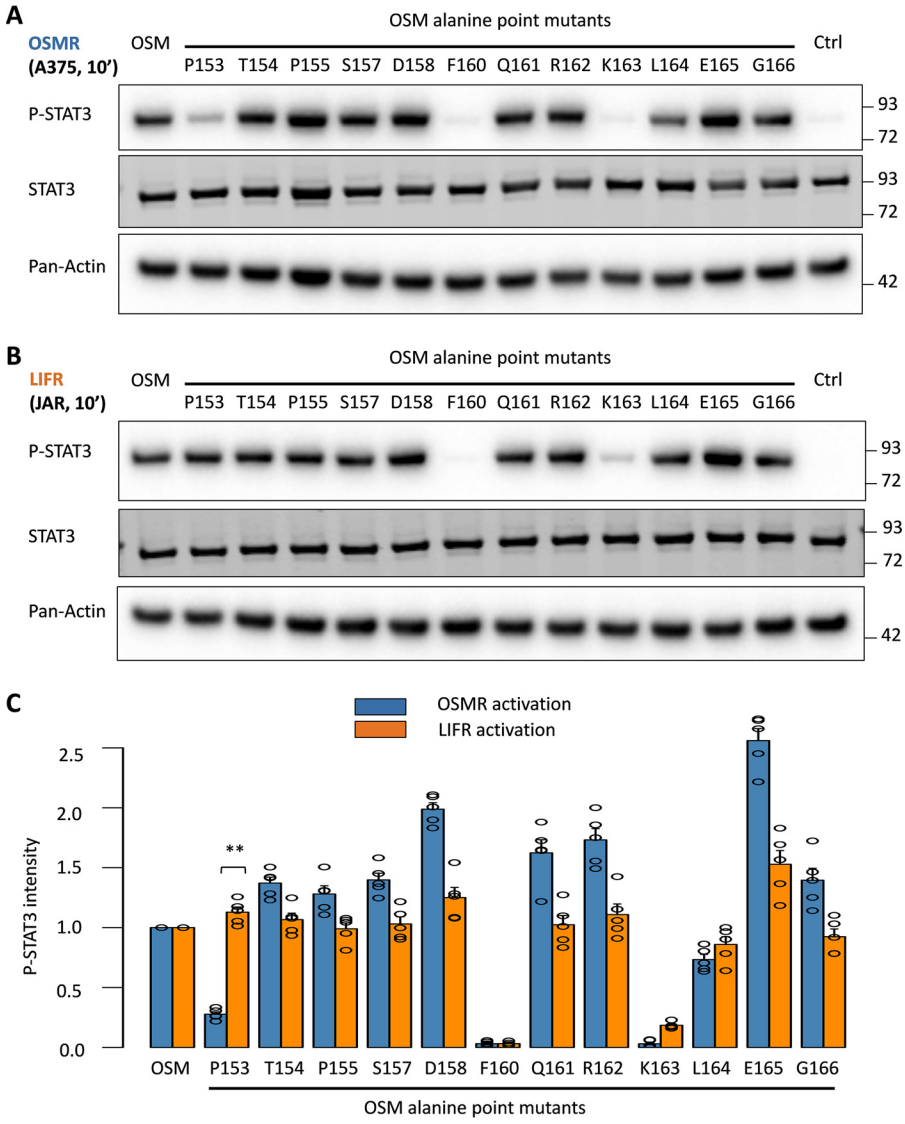

Figure 8. Specific residues in the D-helix of OSM determine short-term receptor activation. *A* and *B*, STAT3 phosphorylation levels in A375 cells (OSMR activity) and JAR cells (LIFR activity) 10 min after stimulation with OSM D-helix alanine point mutants. *Ctrl*, control. *C*, relative quantification of receptor activation by each point mutant. P-STAT3 band intensities were first normalized against total STAT3 levels. Data were then transformed relative to the basal (control) signal, which was set to 0. Values are presented as mean ± S.E., $n = 5$ independent cultures; **, $p < 0.01$.

rected mutagenesis of OSM was performed by full-plasmid amplification, using overlapping primers containing the desired mutation and PfuUltra High Fidelity DNA polymerase (catalog no. 600380, Agilent). Prokaryotic expression constructs were used as templates to generate mammalian expression constructs. To this end, the respective gene sequences accompanied by the His_6 tag were amplified with PacI and AscI restriction sites and cloned into a pCAG-GS vector. All constructs were verified by DNA sequencing. For a complete list of primers used, see Table S1.

Protein expression and purification

Prokaryotic expression plasmids were transformed into SHuffle T7 Express-competent *E. coli* (catalog no. C3029H, New England Biolabs). Transformed cells were grown at 30 °C, and protein expression was induced at an A_{600} of 0.5–0.6 by addition of 0.1 mM isopropyl 1-thio-β-D-galactopyranoside. After 4–6 h of incubation, bacteria were harvested by centrifugation and sonicated following standard protocols.

Eukaryotic expression was achieved in shaking cultures of FreeStyle 293-F cells (catalog no. R79007, Thermo Fisher Scientific) according to the manufacturer's instructions. The supernatants were harvested 3 days after transfection for OSM-based cytokines and 7 days after transfection for LIF-derived cytokines. Both prokaryotically and eukaryotically derived cytokines were then subjected to nickel-nitrilotriacetic acid affinity purification using standard procedures.

Cell lines

A375 cells (catalog no. 88113005) were purchased from the European Collection of Authenticated Cell Cultures. JAR cells (catalog no. ATCC HTB-144) were purchased from the American Type Culture Collection. HepG2 cells were a kind gift from Dr. Sarah Tonack (Max Planck Institute for Heart and Lung Research).

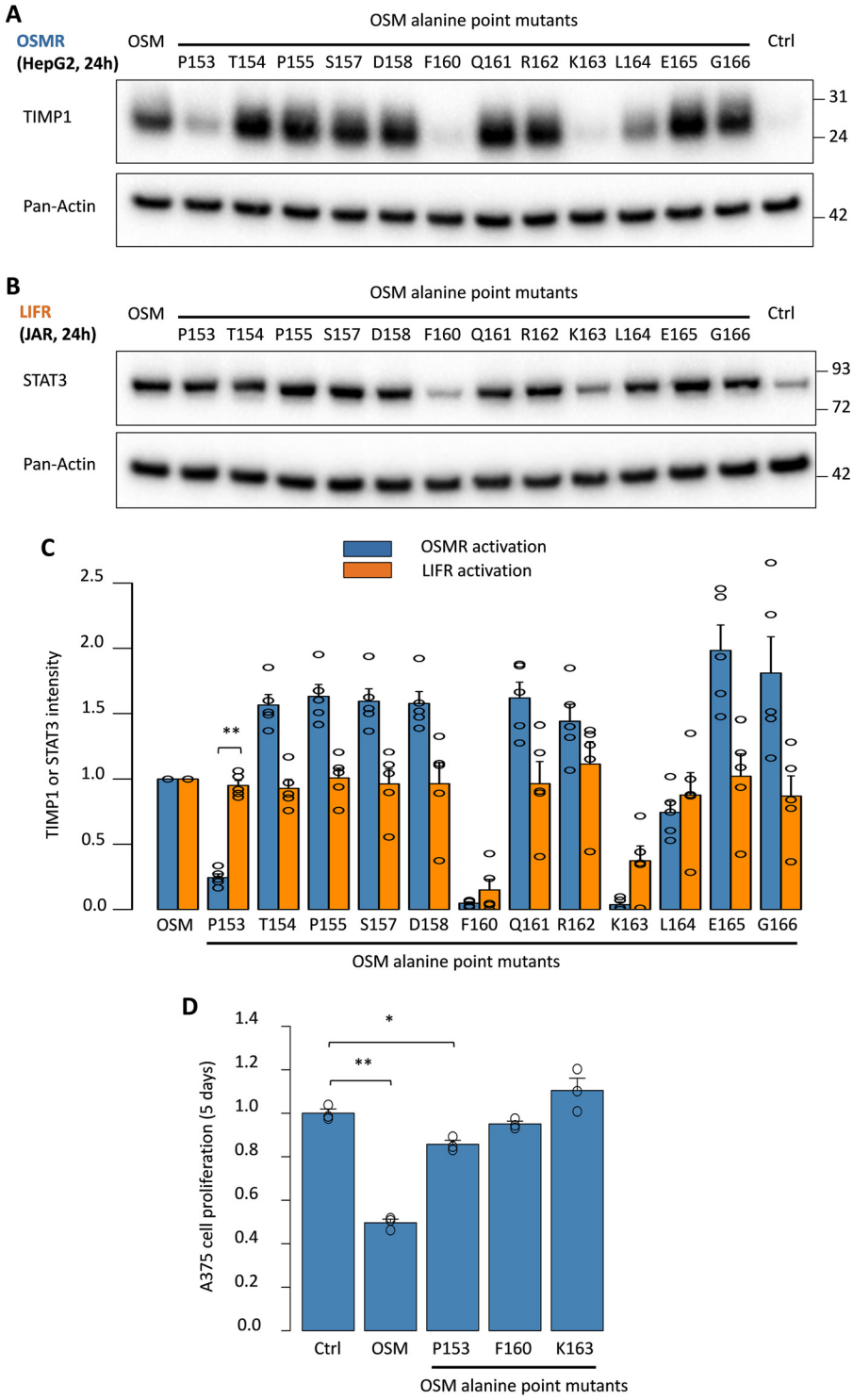

Figure 9. Point mutations in particular OSM D-helix residues modify long-term receptor activation. *A* and *B*, TIMP1 levels in HepG2 cells (OSMR activity) and STAT3 levels in JAR cells (LIFR activity) 24 h after OSM D-helix alanine point mutant stimulation. *Ctrl*, control. *C*, relative quantification of receptor activation by each point mutant. TIMP1 and STAT3 band intensities were first normalized against pan-Actin levels. Data were then transformed relative to the basal (control) signal, which was set to 0. Values are presented as mean ± S.E., $n = 5$ independent cultures; **, $p < 0.01$. *D*, A375 cell proliferation after 5-day cytokine stimulation with selected alanine point mutants, normalized to the proliferation of untreated cells. Values are presented as mean ± S.E., $n = 3$ independent cultures; *, $p < 0.05$; **, $p < 0.01$.

Cell culture conditions and cytokine stimulations

A375 cells were cultured in DMEM, JAR cells in RPMI 1640 medium, and HepG2 cells in DMEM/F12 medium obtained from Gibco, in all cases supplemented with 10% fetal bovine serum, penicillin, and streptomycin (Sigma-Aldrich). The presence of serum did not interfere with the readout systems employed in stimulations experiments; hence, no serum depletion was performed. Cytokines were added at a final concentration of 25 ng/ml to subconfluent cells (~80% confluent in 10-min stimulations, 60% in 24-h experiments), after which

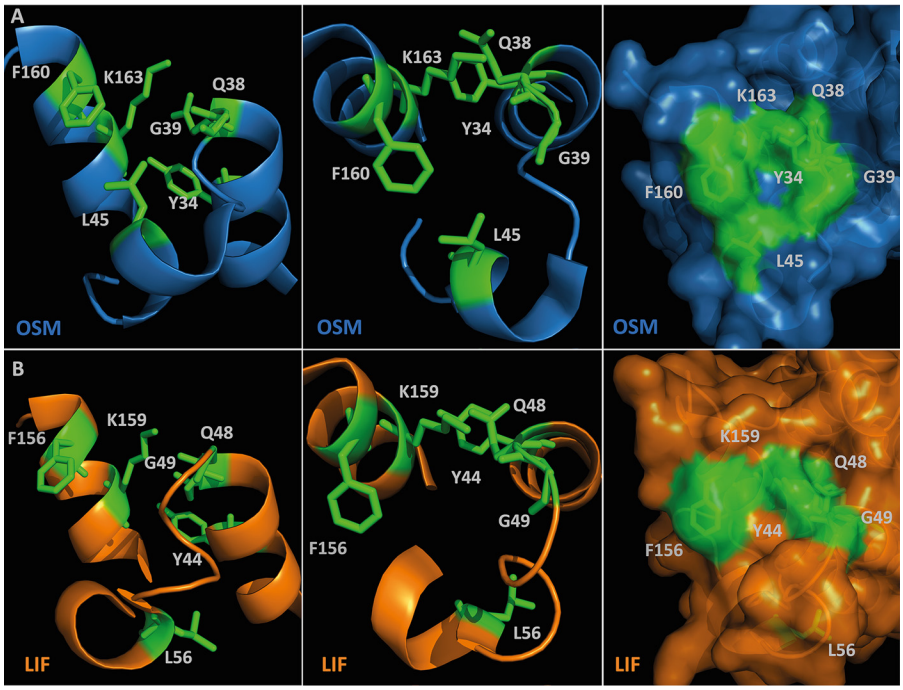

Figure 10. Conservation of AB loop and D-helix regions in OSM and LIF. *A* and *B*, the crystal structures of OSM (*A*, PDB code 1EVS) and LIF (*B*, PDB code 2Q7N) are shown in two different orientations, accompanied by a surface rendering, with the conserved residues critical for OSMR activation highlighted in *green*. Protein structures were visualized with MacPyMOL.

cells were returned to the 37 °C incubator (humidified atmosphere, 5% CO_2) for the duration of the stimulation. Proteins were isolated, quantified, and prepared for SDS-PAGE electrophoresis following standard protocols.

Immunoblots

10 μg of protein for each sample was electrophoresed in NuPAGE 4–12% BisTris protein gels (Novex), and separated proteins were transferred to nitrocellulose membranes (Amersham Biosciences). Membranes were probed with antibodies against phospho-STAT3 (Tyr-705) (catalog no. 9131, lot 30, Cell Signaling Technology), pan-Actin (catalog no. 4968, lot 3, Cell Signaling Technology), TIMP1 (catalog no. 8946, lot 1, Cell Signaling Technology), or total STAT3 (catalog no. 9139, lot 8, Cell Signaling Technology). Bands were detected by means of HRP-conjugated secondary antibodies using the West Femto substrate (catalog no. 34095, Thermo Fisher Scientific) and a ChemiDoc MP System (Bio-Rad). Band intensity was quantified using the Image Lab software (version 5.0, Bio-Rad).

In the case of membranes blotted against phospho-STAT3 (Tyr-705), the same membrane was reblocked and probed against total STAT3. Total STAT3 levels were detected using an Alexa Fluor 680–conjugated secondary antibody (catalog no. A21057, Invitrogen) with the Odyssey® 9120 imaging system (LI-COR Biosciences) and quantified with Image Studio (version 4.0.21, LI-COR Biosciences).

Cell proliferation assays

A375 cells were seeded in 96-well cell culture plates at a density of 5000 cells/well in DMEM without phenol red. After addition of 10 ng/ml cytokine, cells were allowed to grow for 5 days before measuring cell proliferation using the Vybrant 3-(4,5-dimethylthiazol-2-yl)-2,5-diphenyltetrazolium bromide cell proliferation assay kit (catalog no. V13154, Thermo Fisher Scientific).

Statistical analysis

Differences between the groups were assessed by means of a two-tailed Welch's *t* test, considering *p* values below 0.05 to be significant. All analyses were performed using R (version 3.0.3, The R Foundation for Statistical Computing) and RStudio (version 0.98.1062, RStudio).

Structural visualization

Protein structures were visualized using MacPyMOL (version 1.7.2.1, Schrödinger LLC), using available crystal structure data for human OSM (PDB code 1EVS) and human LIF (PDB code 2Q7N). Surface charge was compared using PDB2PQR (version 2.1.1) and the APBS plugin (version 2.1) for MacPyMOL (59, 60).

Author contributions—J. M. A.-S., T. B., and J. P. conceptualization; J. M. A.-S. investigation; J. M. A.-S., N. S., P. G., and H. L. methodology; J. M. A.-S., T. B., and J. P. writing-original draft; P. G., H. L., T. B., and J. P. writing-review and editing; T. B. and J. P. supervision.

Acknowledgments—We thank Jutta Wetzel and Kerstin Richter for excellent technical assistance. We also thank Dr. André Schneider for the gift of the pCAG-GS plasmid, Dr. Heike Hermanns (Division of Hepatology, University Hospital Würzburg) for contributing human OSM cDNA, and Dr. Sarah Tonack for providing the HepG2 cell line.

References

1. Hirano, T., Taga, T., Nakano, N., Yasukawa, K., Kashiwamura, S., Shimizu, K., Nakajima, K., Pyun, K. H., and Kishimoto, T. (1985) Purification to

homogeneity and characterization of human B-cell differentiation factor (BCDF or BSFp-2). *Proc. Natl. Acad. Sci. U.S.A.* **82,** 5490–5494 CrossRef Medline
2. Ip, N. Y., Nye, S. H., Boulton, T. G., Davis, S., Taga, T., Li, Y., Birren, S. J., Yasukawa, K., Kishimoto, T., and Anderson, D. J. (1992) CNTF and LIF act on neuronal cells via shared signaling pathways that involve the IL-6 signal transducing receptor component gp130. *Cell* **69,** 1121–1132 CrossRef Medline
3. Gearing, D. P., Comeau, M. R., Friend, D. J., Gimpel, S. D., Thut, C. J., McGourty, J., Brasher, K. K., King, J. A., Gillis, S., and Mosley, B. (1992) The IL-6 signal transducer, gp130: an oncostatin M receptor and affinity converter for the LIF receptor. *Science* **255,** 1434–1437 CrossRef Medline
4. Yin, T., Taga, T., Tsang, M. L., Yasukawa, K., Kishimoto, T., and Yang, Y. C. (1993) Involvement of IL-6 signal transducer gp130 in IL-11-mediated signal transduction. *J. Immunol.* **151,** 2555–2561 Medline
5. Pennica, D., Shaw, K. J., Swanson, T. A., Moore, M. W., Shelton, D. L., Zioncheck, K. A., Rosenthal, A., Taga, T., Paoni, N. F., and Wood, W. I. (1995) Cardiotrophin-1: biological activities and binding to the leukemia inhibitory factor receptor/gp130 signaling complex. *J. Biol. Chem.* **270,** 10915–10922 CrossRef Medline
6. Elson, G. C., Lelièvre, E., Guillet, C., Chevalier, S., Plun-Favreau, H., Froger, J., Suard, I., de Coignac, A. B., Delneste, Y., Bonnefoy, J. Y., Gauchat, J. F., and Gascan, H. (2000) CLF associates with CLC to form a functional heteromeric ligand for the CNTF receptor complex. *Nat. Neurosci.* **3,** 867–872 CrossRef Medline
7. Pflanz, S., Hibbert, L., Mattson, J., Rosales, R., Vaisberg, E., Bazan, J. F., Phillips, J. H., McClanahan, T. K., de Waal Malefyt, R., and Kastelein, R. A. (2004) WSX-1 and glycoprotein 130 constitute a signal-transducing receptor for IL-27. *J. Immunol.* **172,** 2225–2231 CrossRef Medline
8. Derouet, D., Rousseau, F., Alfonsi, F., Froger, J., Hermann, J., Barbier, F., Perret, D., Diveu, C., Guillet, C., Preisser, L., Dumont, A., Barbado, M., Morel, A., deLapeyrière, O., Gascan, H., and Chevalier, S. (2004) Neuropoietin, a new IL-6-related cytokine signaling through the ciliary neurotrophic factor receptor. *Proc. Natl. Acad. Sci. U.S.A.* **101,** 4827–4832 CrossRef Medline
9. Dillon, S. R., Sprecher, C., Hammond, A., Bilsborough, J., Rosenfeld-Franklin, M., Presnell, S. R., Haugen, H. S., Maurer, M., Harder, B., Johnston, J., Bort, S., Mudri, S., Kuijper, J. L., Bukowski, T., Shea, P., *et al.* (2004) Interleukin 31, a cytokine produced by activated T cells, induces dermatitis in mice. *Nat. Immunol.* **5,** 752–760 CrossRef Medline
10. Bazan, J. F. (1990) Haemopoietic receptors and helical cytokines. *Immunol. Today* **11,** 350–354 CrossRef Medline
11. Robinson, R. C., Grey, L. M., Staunton, D., Vankelecom, H., Vernallis, A. B., Moreau, J. F., Stuart, D. I., Heath, J. K., and Jones, E. Y. (1994) The crystal structure and biological function of leukemia inhibitory factor: implications for receptor binding. *Cell* **77,** 1101–1116 CrossRef Medline
12. McDonald, N. Q., Panayotatos, N., and Hendrickson, W. A. (1995) Crystal structure of dimeric human ciliary neurotrophic factor determined by MAD phasing. *EMBO J.* **14,** 2689–2699 Medline
13. Deller, M. C., Hudson, K. R., Ikemizu, S., Bravo, J., Jones, E. Y., and Heath, J. K. (2000) Crystal structure and functional dissection of the cytostatic cytokine oncostatin M. *Structure* **8,** 863–874 CrossRef Medline
14. Heinrich, P. C., Behrmann, I., Müller-Newen, G., Schaper, F., and Graeve, L. (1998) Interleukin-6-type cytokine signalling through the gp130/Jak/STAT pathway. *Biochem. J.* **334,** 297–314 CrossRef Medline
15. Heinrich, P. C., Behrmann, I., Haan, S., Hermanns, H. M., Müller-Newen, G., and Schaper, F. (2003) Principles of interleukin (IL)-6-type cytokine signalling and its regulation. *Biochem. J.* **374,** 1–20 CrossRef Medline
16. Rose, T. M., Lagrou, M. J., Fransson, I., Werelius, B., Delattre, O., Thomas, G., de Jong, P. J., Todaro, G. J., and Dumanski, J. P. (1993) The genes for oncostatin M (OSM) and leukemia inhibitory factor (LIF) are tightly linked on human chromosome 22. *Genomics* **17,** 136–140 CrossRef
17. Jeffery, E., Price, V., and Gearing, D. P. (1993) Close proximity of the genes for leukemia inhibitory factor and oncostatin M. *Cytokine* **5,** 107–111 CrossRef Medline
18. Giovannini, M., Djabali, M., McElligott, D., Selleri, L., and Evans, G. A. (1993) Tandem linkage of genes coding for leukemia inhibitory factor (LIF) and oncostatin M (OSM) on human chromosome 22. *Cytogenet. Cell Genet.* **64,** 240–244 CrossRef Medline
19. Murakami, M., Hibi, M., Nakagawa, N., Nakagawa, T., Yasukawa, K., Yamanishi, K., Taga, T., and Kishimoto, T. (1993) IL-6-induced homodimerization of gp130 and associated activation of a tyrosine kinase. *Science* **260,** 1808–1810 CrossRef Medline
20. Mosley, B., De Imus, C., Friend, D., Boiani, N., Thoma, B., Park, L. S., and Cosman, D. (1996) Dual oncostatin M (OSM) receptors. Cloning and characterization of an alternative signaling subunit conferring OSM-specific receptor activation. *J. Biol. Chem.* **271,** 32635–32643 CrossRef Medline
21. Chollangi, S., Mather, T., Rodgers, K. K., and Ash, J. D. (2012) A unique loop structure in oncostatin M determines binding affinity toward oncostatin M receptor and leukemia inhibitory factor receptor. *J. Biol. Chem.* **287,** 32848–32859 CrossRef Medline
22. Hermanns, H. M. (2015) Oncostatin M and interleukin-31: cytokines, receptors, signal transduction and physiology. *Cytokine Growth Factor Rev.* **26,** 545–558 CrossRef Medline
23. Hudson, K. R., Vernallis, A. B., and Heath, J. K. (1996) Characterization of the receptor binding sites of human leukemia inhibitory factor and creation of antagonists. *J. Biol. Chem.* **271,** 11971–11978 CrossRef Medline
24. Kallen, K. J., Grötzinger, J., Lelièvre, E., Vollmer, P., Aasland, D., Renné, C., Müllberg, J., Myer zum Büschenfelde, K. H., Gascan, H., and Rose-John, S. (1999) Receptor recognition sites of cytokines are organized as exchangeable modules: transfer of the leukemia inhibitory factor receptor-binding site from ciliary neurotrophic factor to interleukin-6. *J. Biol. Chem.* **274,** 11859–11867 CrossRef Medline
25. Huyton, T., Zhang, J.-G., Luo, C. S., Lou, M.-Z., Hilton, D. J., Nicola, N. A., and Garrett, T. P. (2007) An unusual cytokine:Ig-domain interaction revealed in the crystal structure of leukemia inhibitory factor (LIF) in complex with the LIF receptor. *Proc. Natl. Acad. Sci. U.S.A.* **104,** 12737–12742 CrossRef Medline
26. Sievers, F., Wilm, A., Dineen, D., Gibson, T. J., Karplus, K., Li, W., Lopez, R., McWilliam, H., Remmert, M., Söding, J., Thompson, J. D., and Higgins, D. G. (2011) Fast, scalable generation of high-quality protein multiple sequence alignments using Clustal Omega. *Mol. Syst. Biol.* **7,** 539 Medline
27. Sporeno, E., Barbato, G., Graziani, R., Pucci, P., Nitti, G., and Paonessa, G. (1994) Production and structural characterization of amino terminally histidine tagged human oncostatin M in *E. coli*. *Cytokine* **6,** 255–264 CrossRef Medline
28. Kallestad, J. C., Shoyab, M., and Linsley, P. S. (1991) Disulfide bond assignment and identification of regions required for functional activity of oncostatin M. *J. Biol. Chem.* **266,** 8940–8945 Medline
29. de Marco, A. (2009) Strategies for successful recombinant expression of disulfide bond-dependent proteins in *Escherichia coli*. *Microb. Cell Fact.* **8,** 26 CrossRef Medline
30. Wang, Y., Robledo, O., Kinzie, E., Blanchard, F., Richards, C., Miyajima, A., and Baumann, H. (2000) Receptor subunit-specific action of oncostatin M in hepatic cells and its modulation by leukemia inhibitory factor. *J. Biol. Chem.* **275,** 25273–25285 CrossRef Medline
31. Hermanns, H. M., Radtke, S., Haan, C., Schmitz-Van de Leur, H., Tavernier, J., Heinrich, P. C., and Behrmann, I. (1999) Contributions of leukemia inhibitory factor receptor and oncostatin M receptor to signal transduction in heterodimeric complexes with glycoprotein 130. *J. Immunol.* **163,** 6651–6658 Medline
32. Auguste, P., Guillet, C., Fourcin, M., Olivier, C., Veziers, J., Pouplard-Barthelaix, A., Gascan, H. (1997) Signaling of type II oncostatin M receptor. *J. Biol. Chem.* **272,** 15760–15764 CrossRef Medline
33. Richards, C. D., Shoyab, M., Brown, T. J., and Gauldie, J. (1993) Selective regulation of metalloproteinase inhibitor (TIMP-1) by oncostatin M in fibroblasts in culture. *J. Immunol.* **150,** 5596–5603 Medline
34. Bugno, M., Graeve, L., Gatsios, P., Koj, A., Heinrich, P. C., Travis, J., and Kordula, T. (1995) Identification of the interleukin-6/oncostatin M response element in the rat tissue inhibitor of metalloproteinases-1 (TIMP-1) promoter. *Nucleic Acids Res.* **23,** 5041–5047 CrossRef Medline
35. Zarling, J. M., Shoyab, M., Marquardt, H., Hanson, M. B., Lioubin, M. N., and Todaro, G. J. (1986) Oncostatin M: a growth regulator produced by

differentiated histiocytic lymphoma cells. *Proc. Natl. Acad. Sci. U.S.A.* **83,** 9739–9743 CrossRef Medline
36. Cunningham, B. C., and Wells, J. A. (1989) High-resolution epitope mapping of hGH-receptor interactions by alanine-scanning mutagenesis. *Science* **244,** 1081–1085 CrossRef Medline
37. Plun-Favreau, H., Perret, D., Diveu, C., Froger, J., Chevalier, S., Lelièvre, E., Gascan, H., and Chabbert, M. (2003) Leukemia inhibitory factor (LIF), cardiotrophin-1, and oncostatin M share structural binding determinants in the immunoglobulin-like domain of LIF receptor. *J. Biol. Chem.* **278,** 27169–27179 CrossRef Medline
38. Betts, M. J., and Russell, R. B. (2003) in *Bioinformatics for Geneticists* (Barnes, M. R., and Gray, I. C.) pp. 289–316, John Wiley & Sons, Ltd., Chichester, UK
39. Eisenberg, D., Schwarz, E., Komaromy, M., and Wall, R. (1984) Analysis of membrane and surface protein sequences with the hydrophobic moment plot. *J. Mol. Biol.* **179,** 125–142 CrossRef Medline
40. Khrustalev, V. V., and Barkovsky, E. V. (2012) Stabilization of secondary structure elements by specific combinations of hydrophilic and hydrophobic amino acid residues is more important for proteins encoded by GC-poor genes. *Biochimie* **94,** 2706–2715 CrossRef Medline
41. Drechsler, J., Grötzinger, J., and Hermanns, H. M. (2012) Characterization of the rat oncostatin M receptor complex which resembles the human, but differs from the murine cytokine receptor. *PLoS ONE* **7,** e43155 CrossRef Medline
42. Ichihara, M., Hara, T., Kim, H., Murate, T., and Miyajima, A. (1997) Oncostatin M and leukemia inhibitory factor do not use the same functional receptor in mice. *Blood* **90,** 165–173 Medline
43. Walker, E. C., Johnson, R. W., Hu, Y., Brennan, H. J., Poulton, I. J., Zhang, J.-G., Jenkins, B. J., Smyth, G. K., Nicola, N. A., and Sims, N. A. (2016) Murine oncostatin M acts via leukemia inhibitory factor receptor to phosphorylate signal transducer and activator of transcription 3 (STAT3) but Not STAT1, an effect that protects bone mass. *J. Biol. Chem.* **291,** 21703–21716 CrossRef Medline
44. Tanaka, M., Hirabayashi, Y., Sekiguchi, T., Inoue, T., Katsuki, M., and Miyajima, A. (2003) Targeted disruption of oncostatin M receptor results in altered hematopoiesis. *Blood* **102,** 3154–3162 CrossRef Medline
45. Levy, G., Bomze, D., Heinz, S., Ramachandran, S. D., Noerenberg, A., Cohen, M., Shibolet, O., Sklan, E., Braspenning, J., and Nahmias, Y. (2015) Long-term culture and expansion of primary human hepatocytes. *Nat. Biotechnol.* **33,** 1264–1271 CrossRef Medline
46. Grove, R. I., Mazzucco, C. E., Radka, S. F., Shoyab, M., and Kiener, P. A. (1991) Oncostatin M up-regulates low density lipoprotein receptors in HepG2 cells by a novel mechanism. *J. Biol. Chem.* **266,** 18194–18199 Medline
47. Richards, C. D., Brown, T. J., Shoyab, M., Baumann, H., and Gauldie, J. (1992) Recombinant oncostatin M stimulates the production of acute phase proteins in HepG2 cells and rat primary hepatocytes *in vitro*. *J. Immunol.* **148,** 1731–1736 Medline
48. Guihard, P., Danger, Y., Brounais, B., David, E., Brion, R., Delecrin, J., Richards, C. D., Chevalier, S., Rédini, F., Heymann, D., Gascan, H., and Blanchard, F. (2012) Induction of osteogenesis in mesenchymal stem cells by activated monocytes/macrophages depends on oncostatin M signaling. *Stem Cells* **30,** 762–772 CrossRef Medline
49. Richards, C. D. (2013) The enigmatic cytokine oncostatin m and roles in disease. *ISRN Inflamm.* **2013,** 512103 Medline
50. Kubin, T., Pöling, J., Kostin, S., Gajawada, P., Hein, S., Rees, W., Wietelmann, A., Tanaka, M., Lörchner, H., Schimanski, S., Szibor, M., Warnecke, H., and Braun, T. (2011) Oncostatin M is a major mediator of cardiomyocyte dedifferentiation and remodeling. *Cell Stem Cell.* **9,** 420–432 CrossRef Medline
51. Sun, D., Li, S., Wu, H., Zhang, M., Zhang, X., Wei, L., Qin, X., and Gao, E. (2015) Oncostatin M (OSM) protects against cardiac ischaemia/reperfusion injury in diabetic mice by regulating apoptosis, mitochondrial biogenesis and insulin sensitivity. *J. Cell. Mol. Med.* **19,** 1296–1307 CrossRef Medline
52. Zhang, X., Zhu, D., Wei, L., Zhao, Z., Qi, X., Li, Z., and Sun, D. (2015) OSM enhances angiogenesis and improves cardiac function after myocardial infarction. *Biomed. Res. Int.* **2015,** 317905 Medline
53. Guo, S., Li, Z.-Z., Gong, J., Xiang, M., Zhang, P., Zhao, G.-N., Li, M., Zheng, A., Zhu, X., Lei, H., Minoru, T., and Li, H. (2015) Oncostatin M confers neuroprotection against ischemic stroke. *J. Neurosci.* **35,** 12047–12062 CrossRef Medline
54. Hu, J., Zhang, L., Zhao, Z., Zhang, M., Lin, J., Wang, J., Yu, W., Man, W., Li, C., Zhang, R., Gao, E., Wang, H., and Sun, D. (2017) OSM mitigates post-infarction cardiac remodeling and dysfunction by up-regulating autophagy through Mst1 suppression. *Biochim. Biophys. Acta* **1863,** 1951–1961 CrossRef Medline
55. West, N. R., Hegazy, A. N., Owens, B. M. J., Bullers, S. J., Linggi, B., Buonocore, S., Coccia, M., Görtz, D., This, S., Stockenhuber, K., Pott, J., Friedrich, M., Ryzhakov, G., Baribaud, F., Brodmerkel, C., *et al.* (2017) Oncostatin M drives intestinal inflammation and predicts response to tumor necrosis factor-neutralizing therapy in patients with inflammatory bowel disease. *Nat. Med.* **23,** 579–589 Medline
56. Jahani-Asl, A., Yin, H., Soleimani, V. D., Haque, T., Luchman, H. A., Chang, N. C., Sincennes, M.-C., Puram, S. V., Scott, A. M., Lorimer, I. A., Perkins, T. J., Ligon, K. L., Weiss, S., Rudnicki, M. A., and Bonni, A. (2016) Control of glioblastoma tumorigenesis by feed-forward cytokine signaling. *Nat. Neurosci.* **19,** 798–806 CrossRef Medline
57. Pöling, J., Gajawada, P., Richter, M., Lörchner, H., Polyakova, V., Kostin, S., Shin, J., Boettger, T., Walther, T., Rees, W., Wietelmann, A., Warnecke, H., Kubin, T., and Braun, T. (2014) Therapeutic targeting of the oncostatin M receptor-β prevents inflammatory heart failure. *Basic Res. Cardiol.* **109,** 396 CrossRef Medline
58. Dreuw, A., Radtke, S., Pflanz, S., Lippok, B. E., Heinrich, P. C., and Hermanns, H. M. (2004) Characterization of the signaling capacities of the novel gp130-like cytokine receptor. *J. Biol. Chem.* **279,** 36112–36120 CrossRef Medline
59. Dolinsky, T. J., Czodrowski, P., Li, H., Nielsen, J. E., Jensen, J. H., Klebe, G., and Baker, N. A. (2007) PDB2PQR: expanding and upgrading automated preparation of biomolecular structures for molecular simulations. *Nucleic Acids Res.* **35,** W522–W525 CrossRef Medline
60. Baker, N. A., Sept, D., Joseph, S., Holst, M. J., and McCammon, J. A. (2001) Electrostatics of nanosystems: application to microtubules and the ribosome. *Proc. Natl. Acad. Sci. U.S.A.* **98,** 10037–10041 CrossRef Medline